Identification of hydrogen configurations in *p*-type GaN through first-principles calculations of vibrational frequencies

Sukit Limpijumnong,* John E. Northrup, and Chris G. Van de Walle
Palo Alto Research Center, 3333 Coyote Hill Road, Palo Alto, California 94304, USA
(Received 1 May 2003; published 21 August 2003)

We present first-principles calculations for stable and metastable geometries of various hydrogen-related configurations in *p*-type GaN, including isolated interstitial H as well as Mg-H and Be-H complexes. We also calculate the associated vibrational stretching and wagging modes, systematically including anharmonic contributions to the vibrational frequencies; the anharmonicity is large due to the light mass of the hydrogen atom. Based on our investigations of a large number of configurations we derive a correlation between the vibrational frequency of the stretching mode and the bond length in the N-H bond. The results are compared with experimental results; in particular, we address a new configuration for the Mg-H complex that agrees with the geometrical information extracted from polarization-dependent infrared spectroscopy [B. Clerjaud *et al.*, Phys. Rev. B **61**, 8328 (2000)].

DOI: 10.1103/PhysRevB.68.075206 PACS number(s): 61.72.Bb, 61.72.Vv, 63.20.Pw

I. INTRODUCTION

Hydrogen is abundantly present in the growth environment of many of the commonly used techniques to grow GaN, such as metal-organic chemical vapor deposition (MOCVD), hydride vapor-phase epitaxy (HVPE), or molecular beam epitaxy (MBE) when NH_3 is used as a source gas. Hydrogen readily incorporates in *p*-type GaN, acting as a donor and exhibiting high solubility as well as high diffusivity (the calculated migration barrier is 0.7 eV).[1] Magnesium-hydrogen complexes form during cool down, and the resulting deactivation of the acceptors explains the need for a post-growth activation treatment.[2,3]

Knowledge of the atomic configurations in which hydrogen appears before, during, and after the activation process would be very helpful for optimizing the activation process, and various experimental studies have been devoted to this issue.[4–6] Most of the information has been obtained with vibrational spectroscopy, which measures frequencies of the local vibrational modes of the hydrogen-related configurations. These experiments therefore do not provide direct information about the microscopic structure. In order to obtain such information, the experimental results must be combined with computational studies of the type reported in the present work.

We have carried out first-principles calculations for a variety of hydrogen-related configurations, and identified stable and metastable configurations for isolated interstitial H^+ GaN, as well as for Mg-H complexes. In addition, we address Be-doped material, since Be has been identified as a potential alternative acceptor in GaN.[7,8] For each of these configurations we have also calculated the local vibrational modes. Comparison with experiment then allows for an unambiguous microscopic identification of the configuration that gives rise to a particular frequency in the vibrational spectrum.

Calculations of vibrational frequencies for hydrogen-related configurations have been previously reported,[1,9–13] however, anharmonic terms were not included in those calculations. Since hydrogen is a very light atom, such anharmonic terms are sizable. In this paper we address the calculation of these anharmonic terms and systematically evaluate them for all configurations. We will show that, when anharmonicity is included , the calculated frequencies are very close to the available experimental results.

We have predicted the most probable microscopic structures for each hydrogen-related complex in GaN (i.e., isolated H^+, Mg-H, and Be-H) based on their energies. These structures along with their calculated vibrational characteristics (anharmonicity included) are tabulated in Table I with the theoretically predicted most stable structures listed in boldface. For the isolated H^- and the Mg-H complex there are additional microscopic structures for which the calculated formation energies are close (within 0.2 eV at $T=0$) to that of the lowest energy configuration. These structures and their vibrational characteristics are also listed in the table. We will see shortly that the calculated stretching mode frequecies for the Mg-H complex and the NH_3 molecule (which is included as a test case) agree with experiments; the difference between theory and experiment is less than our estimated error bar of 100 cm^{-1}. We can therefore expect our

TABLE I. Listed are the most stable configurations for each complex and their local vibrational mode frequencies as predicted by the calculations. The lowest energy configuration at zero temperature is shown in boldface. Configurations that are close in energy to the lowest energy configuration (within 0.2 eV at $T=0$) are also listed along with their frequencies. The relative stability of the Mg-H OA and AB_N complexes depends on the temperature as discussed in the text.

Complex	Configuration	$\omega_{stretch}$	ω_{wag}
H^+	**BC**	**3453**	**513**
	AB_N	2872	827
Mg-H	**AB_N**	**3045**	**1061**
	OA	3068	1157
Be-H	**BC**	**3299**	**625**
NH_3		**3280**	

predicted frequencies for unmeasured structures (isolated H^+ and Be-H complex) to be of similar accuracy.

To date, the most detailed experimental studies have been carried out in the case of Mg-H complexes. The local vibrational mode of the Mg-H complex was first identified by Götz *et al.*,[4] in MOCVD-grown films using infrared absorption spectroscopy. They obtained a mode at 3125 cm^{-1}, and correlated it with the Mg-H complex by observing the decrease in intensity of this line after a thermal anneal during which the acceptors were activated (and Mg-H complexes were dissociated). More recently, Harima *et al.* performed similar measurements using Raman spectroscopy of Mg-doped GaN films grown by MOCVD,[5] observing a peak at 3123 cm^{-1} which they also attributed to the Mg-H complex. A peak at 3125 cm^{-1} was also observed by Clerjaud *et al.*[6] in infrared spectroscopy on Mg-doped MOCVD films.

The frequency of the mode at 3125 cm^{-1} is much higher than expected for Mg-H bonds. Previous computations[1,14] showed, however, that the hydrogen atom in the Mg-H complex is strongly bonded to a nitrogen neighbor of the Mg atom, explaining the high frequency of the observed vibrational mode. The calculations placed the hydrogen in an antibonding configuration, on the extension of a Mg-N bond. The recent experimental investigation of Mg-H complexes by Clerjaud *et al.*[6] raised doubts about this identification; indeed, by analyzing the polarization dependence Clerjaud *et al.* found that the angle θ between the c axis and the electric dipole induced by the mode is equal to 130°. This angle was not compatible with any of the models for the Mg-H complex that had been previously considered. In the course of our investigations, we have identified a configuration that results in a value of θ in excellent agreement with experiment. We label this new configuration $OA_{\parallel}$ (for "off-axis bond center" in a bond parallel to the c axis), and will devote a detailed discussion to its structural and energetic properties. A preliminary account of some of the results relating to this complex has been published elsewhere.[15]

In Sec. II we discuss our computational approach and methodology for extracting the vibrational frequencies. Section III describes calculations for an NH_3 molecule, which serve both as an illustration and a test of our approach. Section IV contains results for energetics and Sec. V for vibrational frequencies of various configurations of hydrogen in p-type GaN. Section VI, finally, addresses comparisons with previous calculations and with experimental results and Sec. VII summarizes the paper.

II. METHODS

A. First principles calculations

We employ density-functional theory (DFT) in the local density approximation (LDA)[16] and *ab initio* norm-conserving pseudopotentials, with a plane-wave basis set.[17] We use the so-called "nonlinear core correction" (*nlcc*),[18] allowing us to use an energy cutoff of 40 Ry. Explicit inclusion of the Ga $3d$ states leads to very similar results for the hydrogen-related configurations studied here, as was reported in Ref. 19. Additional comparisons between calculations using the *nlcc* vs those using the $3d$ states performed in the context of the present study will be mentioned in Sec. VI A.

All the calculations reported here are for the wurtzite phase of GaN, and were carried out using the computed lattice parameter of bulk wurtzite GaN $a^{th}=3.089$ Å (compared with $a^{exp}=3.19$ Å). We used the ideal c/a ratio of $\sqrt{8/3}$ which is very close to the calculated c/a ratio of 1.633 (experiment: 1.627). A supercell geometry was employed, with supercells containing 32, 72, and 96 atoms.[8] The larger supercells are required in order to obtain converged results for absolute energies; results for total energies and atomic configurations presented in this paper are taken from 96-atom cell calculations. In many cases, however, the 32-atom cell produces atomic geometries which are exceedingly close to those found in 96-atom cell calculations. In those cases, we have used 32-atom cells for extracting the small energy differences needed to calculate vibrational frequencies. Some additional comments about supercell-size convergence are included in Sec. IV A. In the 96-atom cells, at least 46 host atoms were allowed to relax, while in the 32-atom cell 24 atoms were relaxed.

Brillouin-zone integrations were carried out following the Monkhorst-Pack scheme.[20] The k points are generated by a regularly spaced mesh of $n\times n\times n$ within the first Brillouin zone. Some points in this set are related by symmetry; those points that are not related by symmetry are said to be located in the irreducible part of the zone. Convergence tests indicated that a $2\times2\times2$ sampling suffices for our 32-atom supercell resulting in 3 k points in the irreducible part of the zone.

In order to test the accuracy of our method, we performed calculations of the geometry and vibrational frequencies of an ammonia molecule. For this calculation, we placed one NH_3 molecule in a simple cubic supercell of dimension $8\times8\times8$ Å . Brillouin-zone integrations were carried out with two irreducible k points.

B. Calculation of frequencies for local vibrational modes

In order to calculate vibrational frequencies we use the following approach.[21,22] For a given impurity or complex, we start by calculating the atomic configurations and total energies of stable and metastable configurations (global minimum[23] and local minima in the potential energy surface), including relaxation of the host atoms. Our results will show that all of these configurations exhibit formation of a strong N-H bond; we will therefore focus on the vibrational modes of such N-H bonds. In order to investigate the vibrational stretching mode for a given configuration we introduce small displacements of the H atom along the direction of the N-H bond in both positive and negative directions. We typically include about 20 displacements, with magnitudes up to ±30% of the H-N bond length. The change of total energy as a function of distance then results in a potential energy curve from which we can calculate the vibrational frequency.

Note that all of the host atoms are kept fixed in their (relaxed) equilibrium positions when the H is displaced. Since the hydrogen is much lighter than the host atoms, this

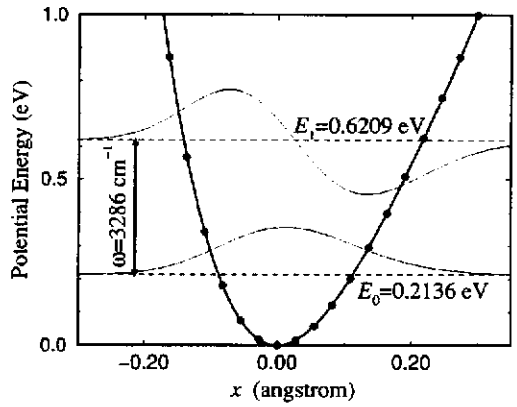

FIG. 1. Calculated potential energy curve for an N-H oscillator, per N-H bond, in the symmetric bond stretch mode of NH_3. The solid circles are calculated results and the solid line is a fourth-order polynomial fit. x is the bond length deviated from the equilibrium position. The reference potential energy is set to zero at the equilibrium position. The energies resulting from a numerical solution to the Schrödinger equation are shown as dashed lines, and the corresponding wave functions are shown in thin solid lines.

is a reasonable approximation. We have investigated the validity of this approximation by explicitly performing calculations in which the N atom to which H is bonded was also allowed to move. We found that displacing only the H atom leads to accurate results (to within 0.5% of the full results), provided the *reduced mass* μ is used in the calculation of the vibrational frequency,[22] where μ is defined as

$$\frac{1}{\mu}=\frac{1}{m_{\mathrm{H}}}+\frac{1}{m_{\mathrm{N}}} \tag{1}$$

with m_{H} and m_{N} the masses of the hydrogen and nitrogen atoms. This yields $\mu=0.9333\ m_{\mathrm{H}}$.

We calculate the vibrational frequencies as follows. The transition energy from the ground state to the first excited state can be written as

$$\Delta E_{0\to 1}=E_1-E_0=\hbar\omega=\hbar(\omega^0+\Delta\omega), \tag{2}$$

where $\Delta\omega$ is the anharmonic contribution and ω is the total frequency. E_0 and E_1 are solutions of the one-dimensional Schrödinger equation

$$\left[-\frac{\hbar^2}{2\mu}\nabla^2+V(x)\right]\psi(x)=E\psi(x). \tag{3}$$

In the simple harmonic approximation ($\alpha=\beta=0$), analytical solutions can be obtained: $E_0=\hbar\omega^0/2$ and $E_1=3\hbar\omega^0/2$, yielding $\Delta E_{0\to 1}=\hbar\omega^0=\sqrt{k/\mu}$. However, for the case at hand the anharmonic terms in the potential are sizable. Indeed, the light mass gives rise to high values of E_0 and E_1 and large vibrational amplitudes, where the potential significantly deviates from a simple parabola (see Fig. 1). We thus resort to an explicit numerical solution of Eq. (3).

We have tested and found that in order to obtain accurate solutions up to E_1, our calculated potential energy values are optimally fit with a fourth degree polynomial, imposing the constraint that the slope of the potential curve is zero at the equilibrium position

$$V(x)=\frac{k}{2}x^2+\alpha x^3+\beta x^4. \tag{4}$$

The coefficient of the quadratic term gives the harmonic frequency, $\omega^0=\sqrt{k/\mu}$, where μ is the reduced mass as defined in Eq. (1). The higher order coefficients α and β describe the anharmonic contributions. The *sweet region* ranges from about 20% bond compression to 30% bond extension. This corresponds to including potential energy values up to at least $\frac{3}{2}\hbar\omega$. Maximum amplitudes smaller than 20% fail to produce reliable fourth-order coefficients, while amplitudes larger than 30% would require fitting to a higher degree polynomial. Our numerical solution of Eq. (3) with the potential given by Eq. (4) is based on the shooting method with 20 000 grid points. We tested the accuracy of this approach in the case of a harmonic potential by comparison with the exact analytic solution. The numerical method introduced an error of less than 5 cm^{-1} in the frequency.

An approximate analytical solution to the Schrödinger equation in the case of an anharmonic potential can be obtained by using perturbation theory[24]

$$\omega=\omega^0+\Delta\omega=\sqrt{\frac{k}{\mu}}-3\frac{\hbar}{\mu}\left[\frac{5}{2}\left(\frac{\alpha}{k}\right)^2-\frac{\beta}{k}\right]. \tag{5}$$

Note that the harmonic term ω^0 is inversely proportional to the square root of the reduced mass μ, while the anharmonic term $\Delta\omega$ is inversely proportional to the reduced mass itself.

For the stretching modes, the perturbation approach yields reasonably good agreement with the numerical results; the frequencies are slightly larger, by about 30 cm^{-1} (worst case: 70 cm^{-1}). As expected, the agreement is good when α/k and β/k are small, and poorer when they are larger (as is the case for wagging modes, see Sec. V C). Overall, the perturbation approach is easier to perform and provides acceptable accuracy. The analytical form of the solutions also helps to assess the relationship between the third- and fourth-order terms in the potential (α and β) and the anharmonic term in the frequency. The explicit comparisons we have performed justify the use of the perturbation approach; however, in the remainder of this paper we will focus on frequencies obtained by explicit numerical solution.

We estimate the error bar on our calculated frequencies to be ± 100 cm^{-1}. One source of error is due to the inherent numerical accuracy (convergence, Brillouin zone sampling, energy cutoff, pseudopotentials, . . .) in the calculation of the potential energy curve. Another source of error is due to the fact that density-functional calculations produce bond lengths that can deviate from experiment by up to one or two percent; this, in turn, can affect the calculated vibrational frequencies. All our tests have indicated that an error bar of ± 100 cm^{-1} is quite conservative.

C. Comparison of frequencies with experiment

Our goal will be to calculate the frequency of N-H stretch modes in various configurations, including both harmonic (ω^0) and anharmonic ($\Delta\omega$) terms, and to compare these with experiment. Experimentally, of course, only the final frequency $\omega=\omega^0+\Delta\omega$ is known. However, there is a way to separate out the anharmonic contributions, namely by comparing the experimental frequencies in deuterated versus hydrogenated systems. By definition, the harmonic frequency is inversely proportional to the square root of the reduced mass. We can thus write

$$\omega_{\mathrm{H}}^0=\sqrt{\frac{\mu_{\mathrm{D}}}{\mu_{\mathrm{H}}}}\omega_{\mathrm{D}}^0. \tag{6}$$

In this expression, μ_{H} and μ_{D} are the appropriate reduced masses of the N-H oscillator and N-D oscillator. Similarly, the anharmonic term is inversely proportional to the reduced mass itself [see Eq. (5)]:

$$\Delta\omega_{\mathrm{H}}=\frac{\mu_{\mathrm{D}}}{\mu_{\mathrm{H}}}\Delta\omega_{\mathrm{D}}. \tag{7}$$

We can also write

$$\omega_H=\omega_H^0+\Delta\omega_H, \tag{8}$$

$$\omega_D=\omega_D^0+\Delta\omega_D. \tag{9}$$

Combining Eqs. (6), (7), (8), and (9) we obtain a system of two linear equations that allows us to solve for ω_{H}^0, $\Delta\omega_{\mathrm{H}}$, ω_{D}^0, and $\Delta\omega_{\mathrm{D}}$.

III. TEST CALCULATIONS FOR NH_3

In order to test the accuracy of our computational approach for calculating vibrational frequencies, and in particular the anharmonic contributions, we wanted to perform a test calculation for a structure for which the frequencies are accurately known experimentally. We chose to do this for the NH_3 molecule. First, we optimized the geometry. Figure 2 shows our calculated relaxed structure compared with the experimental structure. The N-H bond length is 0.6% larger than experiment,[25] while the calculated bond angle is 107.0°, compared with the experimental value of 106.7°.

We performed calculations to determine the frequency of the symmetric stretch mode for NH_3 using our approach for including anharmonic effects and also with the usual harmonic approximation. This allows us to assess the relative importance of the stretch-wag coupling and the anharmonic terms in the potential energy. In the harmonic approximation we may obtain the frequencies for the symmetric stretch and wag modes from a 2×2 dynamical matrix. The two relevant degrees of freedom are $s_1=dr$ and $s_2=r_0d\theta$, as illustrated in Fig. 2. The corresponding force constants are $k_{11}=44.58$ eV/Å, $k_{12}=5.62$ eV/Å, and $k_{22}=8.28$ eV/Å. By solving for the frequency of the symmetric stretch mode with these force constants, and then with $k_{12}=0$, we determined that the effect of including the stretch-wag coupling is to increase the frequency of the stretch mode by 23 cm^{-1}.

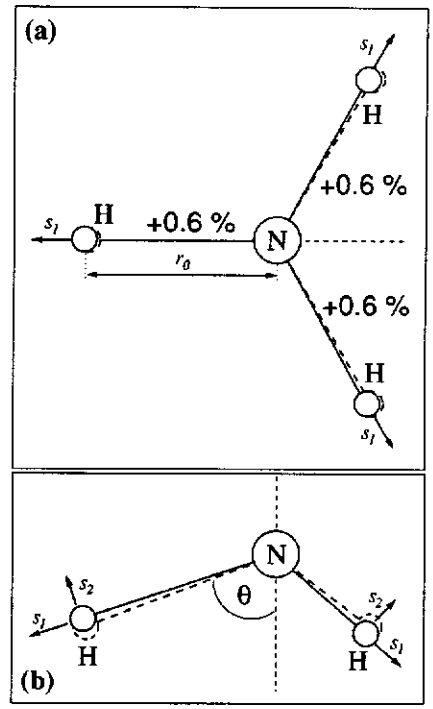

FIG. 2. Calculated structure of NH_3 (solid lines) compared with the experimental structure (dashed lines), (a) Top view, (b) side view, cutting through one of the N-H bonds. N-H distances (r_0) are given as percentage deviations from the experimental value (1.012 Å). The calculated value of θ is 68.2°, the experimental value is 67.9°. s_1 and s_2 are the two degrees of freedom employed in the calculation of the dynamical matrix as discussed in the text.

As we shall see this change in frequency is very small compared to the effect of anharmonicity. To calculate the frequency including anharmonicity we first determine the potential energy $V(s_1)$ resulting from changes in the N-H bond distance while keeping the N-H bond angles fixed. The corresponding kinetic energy in the center-of-mass frame is $T=(1/2)\mu(ds_1/dt)^2$ with $\mu=3m_Hm_N(1+3m_H\sin^2\theta/m_N)/(m_N+3m_H)$. We obtain a value for the stretch frequency by solving Schrödinger's equation numerically with this potential V and with reduced mass μ. The resulting frequency is $\omega_{\mathrm{anharmonic}}=3280$ cm^{-1}. This result differs from the experimental value (3337 cm^{-1}) by only 1.7 %. On the other hand we fit $V(s_1)$ with a quadratic function we obtain $\omega_{\mathrm{harmonic}}=3507$ cm^{-1}. It is clear from this analysis that inclusion of the anharmonicity is quite important while the affect of stretch-wag coupling is small and can be ignored. We expect our approach to yield a similar level of accuracy in the case of the N-H stretch modes discussed later.

Our calculated *harmonic* frequency for the NH_3 symmetric stretching mode is typical of what has been obtained in prior DFT calculations. According to the data base at the National Institute of Standards and Technology (NIST), our harmonic frequency of 3507 cm^{-1} is within the range of frequencies (3425–3575 cm^{-1}) obtained by various methods and basis sets[26] (over 60 sets of different calculations in

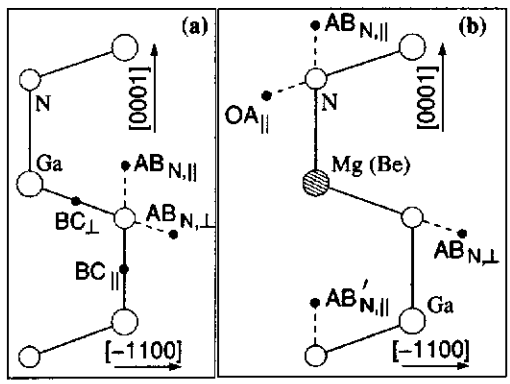

FIG. 3. Schematic representation of possible hydrogen sites in the (11-20) plane of wurtzite GaN. (a) Sites in bulk GaN, (b) sites near a substitutional acceptor (Mg, Be). The large open circles represent Ga atoms, large patterned circle Mg (or Be), medium circles N atoms. The possible sites for H are represented by the small solid circles.

total) ranging from DFT to coupled-cluster, singles, and doubles with approximate triples [CCSD(T)] which is a very expensive approach. Since these calculations are based on the dynamical matrix approach, the anharmonic corrections are not included and the calculated frequency is systematically higher than experiment. We therefore believe that the good agreement between our calculated *anharmonic* frequency and the experimental value is a result of our further treatment of the substantial (-227 cm^{-1}) anharmonic corrections to this particular mode.

IV. ATOMIC STRUCTURE AND ENERGETICS OF HYDROGEN CONFIGURATIONS IN *P*-TYPE WURTZITE GaN

In this section we discuss the stability of isolated interstitial H^-, and of Mg-H and Be-H complexes. In *p*-type GaN (or as long as the Fermi level is within about 2 eV of the valence-band maximum) hydrogen occurs in the positive charge state and prefers interstitial locations close to the nitrogen atom.[1] The presence of hydrogen in the system thus leads to compensation. In addition, electrostatic forces attract H to the acceptor (which is negatively charged when donating a hole to the valence band or when compensated) resulting in the formation of hydrogen-acceptor complexes. We explored various low-energy sites for H, finding that the antibonding nitrogen (AB_N) and bond center (BC) sites are most favorable. In the wurtzite structure, there are two types of each AB_N and BC: one type has threefold symmetry and is associated with bonds oriented parallel to the *c* axis; we label these sites $BC_\parallel$ and $AB_{N,\parallel}$. The other type is associated with the bonds that are *not* parallel to the *c* axis; although these are not exactly "perpendicular" to the *c* axis, we use the notation $BC_\perp$ and $AB_{N,\perp}$. All of these sites are shown in Fig. 3(a). For H near Mg or Be acceptors, there are additional possible configurations for the antibonding site: we label these $AB'_{N,\parallel}$ and $OA_\parallel$, as shown in Fig. 3(b).

TABLE II. Energy differences (eV) between different configurations of H in *p*-type wurtzite GaN; in each case, the lowest energy configuration is used as a reference with zero energy. The results were obtained from 96-atom supercell calculations.

Configuration	H^+	Mg-H	Be-H
$BC_\parallel$	0.00	0.33	0.00
$BC_\perp$	0.13	0.54	0.13
$AB_{N,\parallel}$	0.33	0.28	1.12
$AB_{N,\perp}$	0.13	0.00	0.86
$AB'_{N,\parallel}$		0.73	1.68
$OA_\parallel$		0.19	

A. Isolated interstitial hydrogen

The stable charge state for H in *p*-type GaN is $+1$.[1] In this charge state, H prefers to stay close to the N atom. The energy surface mapped out in earlier work[1] shows that H favors positions on a sphere with a radius of approximately 1 Å centered on a N atom. For cubic GaN, the earlier calculations showed that the energy difference between H^+ at AB_N and BC sites was very small. This qualitative conclusion is confirmed by our present calculations for wurtzite GaN. H^+ prefers the $BC_\parallel$ site, with the energy at $BC_\perp$ and at $AB_{N,\parallel}$ only 0.13 eV higher. Energy differences between the various configurations are listed in Table II. In addition, Table III lists details about the atomic relaxations, and the relaxed structures are shown in Fig. 4. Table III and Fig. 4 reflect results obtained in 96-atom cells; these agree quite well with results from 32-atom cells. For instance, N-H bond lengths agree to within 0.004 Å. We will take advantage of this fact when calculating vibrational frequencies.

Large relaxations of the host atoms occur: for H at the BC sites, the Ga atom moves outward by more than 30% of the bond length, while the N atom moves by 14%. It is quite remarkable that, in spite of this huge relaxation which effectively breaks the original Ga-N bond, hydrogen still favors this site. The reason for this must be that a large amount of energy can be gained in forming the N-H bond. The Ga atom, meanwhile, is pushed into the plane of its three N neighbors.

TABLE III. Calculated energy differences ΔE and lattice relaxations for interstitial H^+ in wurtzite GaN, for various lattice locations. The results were obtained from 96-atom supercell calculations. The global minimum ($BC_\parallel$) is chosen as the zero of energy. $\Delta d_{Ga(N)}$ denotes the displacement of the nearest neighbor Ga(N) atom from its nominal lattice site, expressed as a percentage of the bond length. $d_{Ga\text{-}H}$ denotes the Ga-H distance and $d_{N\text{-}H}$ the N-H distance, in Å.

Configuration	ΔE (eV)	Δd_{Ga}	Δd_N	$d_{Ga\text{-}H}$ (Å)	$d_{N\text{-}H}$ (Å)
$BC_\parallel$	0.00	35.1%	14.5%	1.80	1.026
$BC_\perp$	0.13	31.7%	13.7%	1.73	1.025
$AB_{N,\perp}$	0.13	2.5%	4.2%		1.044
$AB_{N,\parallel}$	0.33	2.7%	2.2%		1.041

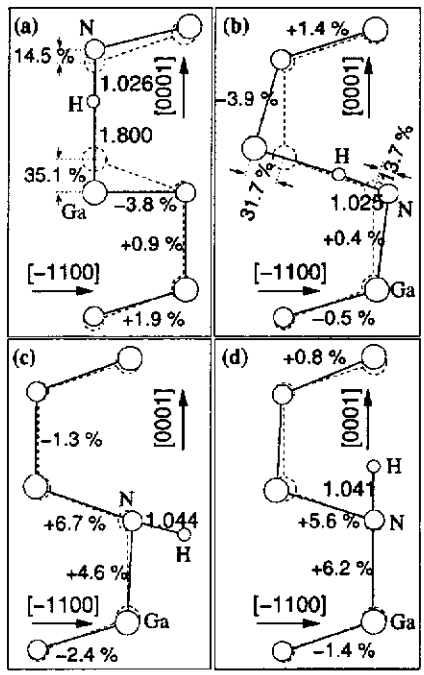

FIG. 4. Schematic representation of atomic positions in the (11-20) plane for H^+ at (a) $BC_{\parallel}$ site, (b) $BC_{\perp}$ site, (c) $AB_{N\perp}$ site, and (d) $AB_{N\parallel}$ site in wurtzite GaN. The configurations are depicted in order of increasing energy (see Table III). Large circles represent Ga atoms, medium circles N atoms, and the small circles H atoms. Dashed circles indicate ideal atomic positions, dashed lines bonds in the ideal lattice. Distances between H and its neighbors are given in Å , changes in Ga-N bond lengths are given as a percentage of change from the bulk Ga-N bond lengths.

For H at AB_N sites, the relaxations are much smaller. As we can see from Fig. 4, the neighboring Ga atoms are pushed slightly outwards from their ideal positions. Hydrogen forms a strong bond with N, causing the bond between this N and the neighboring Ga to be weakened and extended. We will see that this is also true in case of the Mg-H and Be-H complexes.

TABLE IV. Calculated energy differences ΔE and lattice relaxations for Mg-H complexes in wurtzite GaN, for various lattice locations. The results were obtained from 96-atom supercell calculations. The global minimum ($AB_{N\perp}$) is chosen as the zero of energy. Δd_{Mg} denotes the displacement of the Mg atom from its nominal lattice site, and Δd_N the displacement of the N atom to which H is bonded, expressed as a percentage of the bond length. $d_{N\text{-}H}$ denotes the N-H distance in Å.

Configuration	ΔE (eV)	Δd_{Mg}	Δd_N	$d_{N\text{-}H}$ (Å)
$AB_{N\perp}$	0.00	1.7%	14.6%	1.031
$OA_{\parallel}$	0.19	18.0%	10.6%	1.030
$AB_{N\parallel}$	0.28	1.9%	12.2%	1.031
$OA_{\perp}$	0.31	10.9%	10.4%	1.038
$BC_{\parallel}$	0.33	36.9%	13.3%	1.010
$BC_{\perp}$	0.54	39.6%	10.5%	1.006
$AB'_{N\parallel}$	0.73	4.5%	3.9%	1.042

B. Magnesium-hydrogen complexes

We explored seven possible sites for H in GaN:Mg, six of which are depicted in Fig. 3(b), and the seventh is shown in Fig. 5(d). The relative energies are listed in Table II, and details about the atomic relaxations are included in Table IV (all from 96-atom supercells). The relaxed structures are shown in Fig. 5. Generally, the structures relax in a fashion very similar to the corresponding structure for isolated interstitial H^+, with one additional effect: since the Mg-N bond is longer than the Ga-N bond, the N neighbors of Mg are pushed outward, away from the Mg atom. The energy differences show that H favors the antibonding sites, with $AB_{N\perp}$

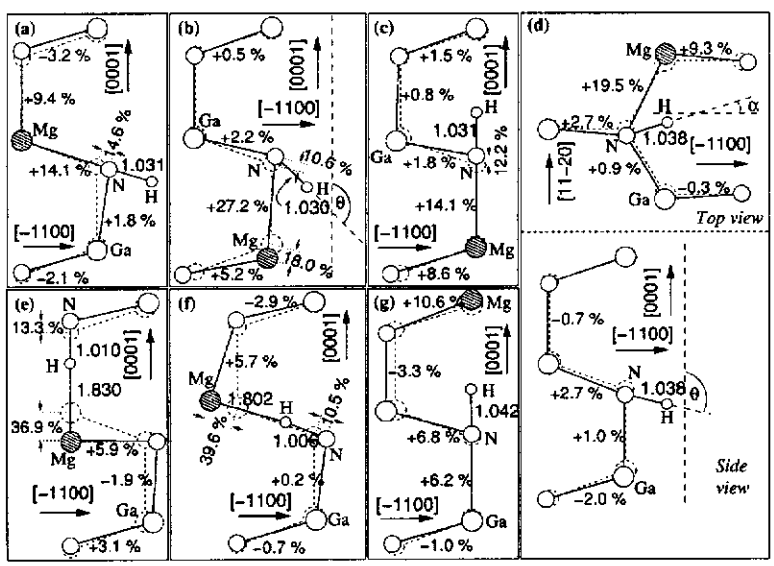

FIG. 5. Schematic representation of atomic positions in the (11-20) plane for a Mg-H complex in wurtzite GaN, with H at the (a) $AB_{N\perp}$ site, (b) $OA_{\parallel}$ site, (c) $AB_{N\parallel}$ site, (d) $OA_{\perp}$ site, (e) $BC_{\parallel}$ site, (f) $BC_{\perp}$ site, and (g) $AB'_{N\parallel}$ site. The configurations are depicted in order of increasing energy (see Table IV). Large circles represent Ga atoms, medium circles N atoms, shaded circle Mg atom, and the small circle H atom. Dashed circles indicate ideal atomic positions, dashed lines bonds in the ideal lattice. Distances between H and its neighbors are given in Å , changes in Ga-N and Mg-N bond lengths are given as a percentage of change from the bulk Ga-N bond lengths.

being the global minimum and $OA_{\parallel}$ only higher by 0.19 eV. We recall that for isolated interstitial H^+ the BC configuration was favored. The difference in the case of the Mg-H complex can be explained on the basis of the larger size of the cation (the covalent radius of Mg is larger than that of Ga, Ref. 27). This larger size renders the BC site less favorable than for isolated interstitial H^-. Hydrogen at the AB_N sites does not suffer from this problem, rendering the AB_N sites more stable than the BC sites. Hydrogen at the $AB'_{N,\parallel}$ site turns out to be least favorable, with an energy 0.73 eV higher than at $AB_{N,\perp}$. The Mg-H complex is barely bound in this configuration, as evidenced by comparison with the calculated binding energy of the Mg-H complex (i.e., the energy difference between H^+ separated by a large distance from Mg^- and the lowest energy of the Mg-H complex), which was previously calculated to be only 0.7 eV.[1] The latter value was obtained for zinc blende; our present calculations in 96-atom wurtzite cells yield a value of 0.77 eV.

A more detailed investigation of the BC configurations reveals that they are actually not even metastable. The results for BC sites included in Tables II and IV and in Fig. 5 were obtained by constraining H to be on the bond axis between the Mg and the N atom (in the case of $BC_{\parallel}$) or in the plane defined by the bond between Mg and N and the c axis (in the case of $BC_{\perp}$). A small displacement away from these BC sites causes H to spontaneously relax to a new configuration, which we label OA (for "off axis"). This relaxation lowers the energy by a few 0.1 eV. There are two types of OA sites: relaxation away from $BC_{\parallel}$ produces $OA_{\parallel}$ [Fig. 5(b)] and relaxation away from $BC_{\perp}$ produces $OA_{\perp}$ [Fig. 5(d)].

An alternative way of looking at the OA configurations is to view them as distorted AB_N configurations. We already found that the $AB_{N,\perp}$ configuration is lowest in energy in the case of the Mg-H complex. The particular configuration depicted in Fig. 5(a) has the Mg atom bonded to the N atom involved in the N-H bond such that the Mg-N and N-H bonds are oriented along the same direction. In this configuration the angle θ between the N-H bond and the c axis is close to 109°. Focusing on the N atom to which the H is bound, there are two other possible positions for the Mg atom as a nearest neighbor of the N atom: the Mg-N bond can be oriented along the c axis [Fig. 5(b)] or it can be oriented along a "perpendicular" direction, but different from the direction of the N-H bond [Fig. 5(d)]. In the latter configuration, the N-H bond is rotated around the c axis by $\alpha=16°$. From Fig. 5 it is clear that the orientation of the N-H bond in the $OA_{\parallel}$ and $OA_{\perp}$ is different from that in the $AB_{N,\perp}$ configuration. In $OA_{\parallel}$, the N-H bond makes a 134° angle with the c axis, while in $OA_{\perp}$ the angle is $\theta=99°$. The relevance of this angle for comparison with experimental data will be discussed in more detail in Sec. VI B.

As can be seen from Table IV the OA complexes are slightly higher in energy than the global minimum, which occurs at $AB_{N,\perp}$. We have recently shown[15] that this slight energy difference (at $T=0$) can be overcome by the large entropy associated with the $OA_{\parallel}$ configuration. At high temperature, which are relevant for the formation of these complexes, the *free energy* of the $OA_{\parallel}$ configuration can thus become lower than that of $AB_{N,\perp}$. We will return to this issue in Sec. VI B.

TABLE V. Calculated energy differences ΔE and lattice relaxations for Be-H complexes in wurtzite GaN, for various lattice locations. The results were obtained from 96-atom supercell calculations. The global minimum ($BC_{\parallel}$) is chosen as the zero of energy. Δd_{Be} denotes the displacement of the Be atom from its nominal lattice site and Δd_N the displacement of the N atom to which H is bonded, expressed as a percentage of the bond length. $d_{N\text{-}H}$ denotes the N-H distance in Å.

Configuration	ΔE (eV)	Δd_{Be}	Δd_N	$d_{N\text{-}H}$ (Å)
$BC_{\parallel}$	0.00	35.3%	10.8%	1.028
$BC_{\perp}$	0.13	31.3%	10.6%	1.027
$AB_{N,\perp}$	0.86	21.2%	12.8%	1.031
$AB_{N,\parallel}$	1.12	23.3%	11.3%	1.030
$AB'_{N,\parallel}$	1.68	3.3%	5.1%	1.059

C. Beryllium-hydrogen complexes

Relative energies for H configurations in the Be-H complex are listed in Table II and details about the atomic relax-

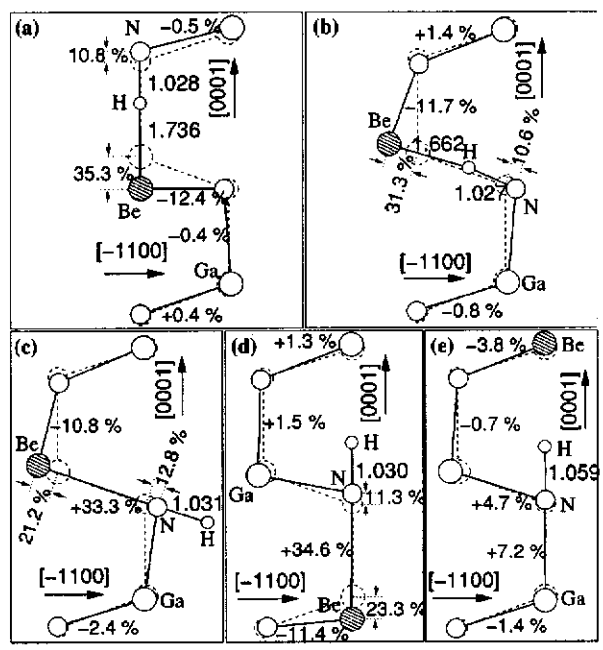

FIG. 6. Schematic representation of atomic positions in the (11-20) plane for a Be-H complex in wurtzite GaN, with H at the (a) $BC_{\parallel}$ site, (b) $BC_{\perp}$ site, (c) $AB_{N,\perp}$ site, (d) $AB_{N,\parallel}$ site, and (e) $AB'_{N,\parallel}$ site. The configurations are depicted in order of increasing energy (see Table V). Large circles represent Ga atoms, medium circles N atoms, shaded circle Be atom, and the small circle H atom. Dashed circles indicate ideal atomic positions, dashed lines bonds in the ideal lattice. Distances between H and its neighbors are given in Å, changes in Ga-N and Be-N bond lengths are given as a percentage of change from the bulk Ga-N bond lengths.

ations are included in Table V. The relaxed structures are shown in Fig. 6. Here, the relative energetic ordering of the configurations is similar to isolated interstitial H^+, although the energy differences between BC and AB sites are larger. Beryllium is a smaller atom than Ga, and the Be-N bond length is smaller than the Ga-N bond length. Therefore, in contrast to Mg, the N atoms surrounding Be are relaxed *inwards*. This smaller size[27] of Be makes it easier for H to assume the BC position, rendering this configuration energetically most favorable. Its energy is roughly 1 eV lower than AB_N. The $AB'_{N,\parallel}$ configuration is again quite close in energy to the configuration where H is fully separated from Be_{Ga}^-; indeed, the binding energy of the Be-H complex is 1.81 eV.[8] Note that the N-H bond length in this complex is 1.059 Å, longer than in any other configuration. We attribute this to an attractive interaction between the Be acceptor and the H atom, combined with the small size of Be. The attractive interaction would also be present in the case of Mg, but there it is balanced by a repulsion due to the large size of Mg, resulting in a N-H bond length very close to that for isolated interstitial H. Finally, we found the OA configurations to be unstable in the case of Be-H; there is no barrier for these configurations to relax towards the corresponding BC configuration.

V. VIBRATIONAL FREQUENCIES

A. Results for stretching modes

In this section, we report our calculated results for vibrational frequencies of N-H bond-stretching modes for many of the configurations mentioned in the previous section. While some of these configurations are much higher in energy than the ground state and are unlikely to occur, they are still useful for studying trends of the N-H modes. Our calculations of vibrational frequencies are carried out in 32-atom cells. As mentioned in Sec. IV A, the accuracy of the calculated relaxations is excellent for most of the configurations in 32-atom cells, with only a few exceptions, in particular in the case of the Mg-H complex. The deviation (compared to 96-atom cells) in the length of the N-H bond is always less than 0.01 Å; however, that amount can make a significant difference in the vibrational frequency. We therefore use 32-atom cell results for those configurations for which the deviation in N-H bond lengths between 32-atom and 96-atom supercells is less than 0.005 Å, which would correspond to an error in the vibrational frequency of less than 100 cm^{-1}. For the configurations that exhibit a larger deviation in the N-H bond length ($AB_{N,\perp}$ and $AB'_{N,\parallel}$), we carried out the vibrational frequency calculations explicitly in 96-atom cells. As we will see in Sec. V B, our results will enable us to establish a strong correlation between vibrational frequencies and bond lengths. Using this correlation, we will then be able to also make predictions for configurations for which the vibrational frequencies were not explicitly calculated.

The potential energy as a function of the N-H vibrational amplitude (x) is shown in Fig. 7 for $BC_\parallel$ positions and in Fig. 8 for $AB_{N,\parallel}$ and $AB'_{N,\parallel}$ positions. In both figures, the potential energy curve for the symmetric stretch mode of NH_3 is included for comparison. Note that the polynomial curves provide excellent fits to the data points, indicative of the high quality of the fit, and also indicating that a fourth-order polynomial suffices to describe the calculated data. The fitting parameters ($k/2$, β, and α) are listed in Table VI, as well as the resulting frequencies, including harmonic (ω^0) and anharmonic ($\Delta\omega$) terms.

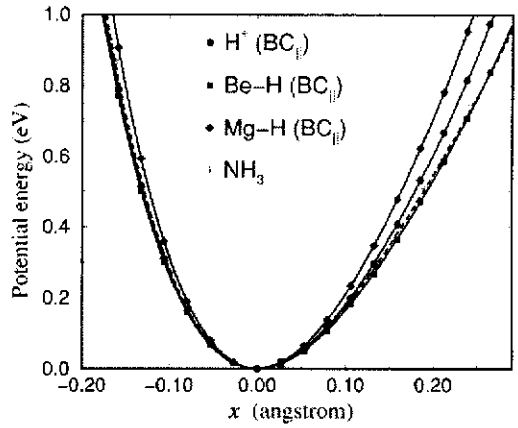

FIG. 7. Calculated potential energy curves for N-H bond-stretching modes for $BC_\parallel$ configurations. The solid symbols are calculated points and the solid lines are the fourth-order polynomial fits [Eq. (4)]. The potential energies are set to zero at the equilibrium position of each structure. The star symbols and dashed line indicate the potential energy curve for the NH_3 symmetric stretch mode, included for comparison.

The potentials for H at BC positions are steeper than at $AB_{N\parallel}$ positions, due to the fact that space is more limited at the BC site, resulting in a stiffening of the N-H bond. This

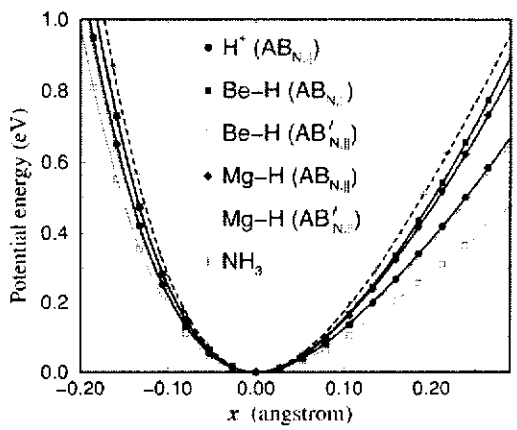

FIG. 8. Calculated potential energy curves for N-H bond-stretch modes for $AB_{N,\parallel}$ and $AB'_{N,\parallel}$ configurations. Solid symbols are calculated points for H at the $AB_{N,\parallel}$ site and the thick solid lines are the corresponding fourth-order polynomial fits [Eq. (4)]. Open symbols and thin solid lines are the calculated points and fits for H at the $AB'_{N,\parallel}$ site. The potential energies are set to zero at the equilibrium position of each structure. The star symbols and dashed line indicate the potential energy curve for the NH_3 symmetric stretch mode, included for comparison.

TABLE VI. Vibrational properties for H-N bond-stretching modes in various configurations, calculated in 32-atom and 96-atom supercells (see text). Values for NH_3 are included for comparison. $d_{N\text{-}H}$ is the N-H distance, in Å. $k/2$, α, and β are the second, third, and fourth order coefficients in the polynomial fit of the potential-energy curve [see Eq. (4)], in eV/Å^n, where n is the order of the coefficient. ω^0 is the harmonic component of the vibrational frequency $\Delta\omega$ is the anharmonic contribution, and ω is the total frequency: $\omega=\omega^0+\Delta\omega$. All frequencies are in cm^{-1}.

Type	Configuration	$d_{N\text{-}H}$ (Å)	$k/2$	α	β	ω^0	$\Delta\omega$	ω
H^+	$BC_\parallel$	1.027	22.21	−47.71	61.66	3581	−128	3453
H^+	$AB_{N,\perp}$	1.045	17.40	−48.48	57.24	3170	−298	2872
H^+	$AB_{N,\parallel}$	1.045	16.72	−47.74	60.18	3108	−288	2820
Mg-H	$AB_{N,\perp}$	1.031	19.24	−51.11	56.49	3333	−288	3045
Mg-H	$OA_\parallel$	1.032	19.31	−50.51	55.32	3339	−271	3068
Mg-H	$AB_{N,\parallel}$	1.031	19.26	−49.99	62.70	3335	−222	3113
Mg-H	$BC_\parallel$	1.009	25.78	−53.23	64.83	3859	−117	3742
Mg-H	$AB'_{N,\parallel}$	1.042	17.92	−48.32	58.45	3217	−263	2954
Be-H	$BC_\parallel$	1.028	20.95	−50.74	63.23	3478	−179	3299
Be-H	$AB_{N,\parallel}$	1.032	19.63	−49.05	62.25	3367	−195	3172
Be-H	$AB'_{N,\parallel}$	1.064	13.65	−43.73	55.89	2808	−403	2405
NH_3		1.018	22.29	−54.56	58.02	3507	−227	3280

results in higher frequencies for BC than AB_N. The frequency at BC is highest for Mg, the largest cation, and lowest for Be, which is the smallest. The stretching frequency for H at $BC_\parallel$ in the Mg-H complex is as high as 3742 cm^{-1}, which is 629 cm^{-1} higher than in the $AB_{N,\parallel}$ configuration, and 289 cm^{-1} higher than for isolated interstitial H^+ at BC. The extension of the N-H bond for H at BC also leads to a repulsive interaction with the cation, resulting in an increase of the potential energy in the $+x$ direction (see Fig. 7); this reduces the anharmonicity. We expect the reduction in anharmonicity to be largest in the case of Mg (the largest atom), and smallest for Be (the smallest atom); the results in Table VI indeed confirm this trend.

Turning now to the AB_N sites, Fig. 8 shows that for all of the configurations the potential curves are less steep than for NH_3. This is due to the fact that in the AB_N configuration the N-H bond is weakened, because the N atom is now fivefold coordinated, having four bonds to cations and one bond to H. The fivefold coordination causes a weakening of all of these bonds, indicated, for instance, by the fact that all of the bond distances surrounding the N atom are increased. Comparing the various $AB_{N,\parallel}$ sites, we note that the potential energy curve in the case of Mg-H and Be-H is somewhat steeper than for isolated interstitial H^+. This can be attributed to the fact that the bond between N and the acceptor impurities is weaker than a Ga-N bond, possibly due to the fact that the acceptors are more comfortable in a threefold coordination (this is certainly true for Be, see Ref. 8); this weakening can result in a strengthening of the N-H bond.

For H at $AB'_{N,\parallel}$ in the Mg-H complex, the potential energy curve and frequency are similar to those for isolated interstitial H^+ at $AB_{N,\parallel}$, indicating that in this case the presence of the Mg impurity across the interstitial void has little effect on the N-H bond. As noted in Sec. IV C, this may be the net result of balancing the attractive interaction between the Mg acceptor and the H atom, and the repulsion due to the large size of Mg. In the Be-H complex, however, the $AB'_{N,\parallel}$ configuration leads to a significant weakening of the N-H bond and a corresponding lowering of the vibrational frequency. We note, however, that the high energy of this configuration makes its occurrence very unlikely.

B. Trends in vibrational frequencies

In the spirit of our systematic investigation of trends in the vibrational frequencies, we have studied the relation between the frequency and the N-H bond length, as shown in Fig. 9. Most of the results included here are from 32-atom cells except those for which the N-H bond length deviated by

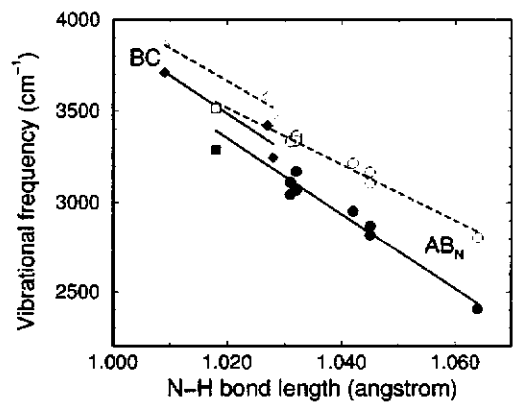

FIG. 9. Calculated vibrational frequencies for various configurations as a function of the N-H bond length. Open symbols indicate harmonic frequencies, solid symbols indicate frequencies including anharmonic contributions. Circles indicate data points from H at AB_N sites listed in Table VI; diamonds indicate data points from H at $BC_\parallel$ sites. The values for the NH_3 symmetric stretch mode are indicated with squares. The solid and dashed lines are linear fits to the data in the corresponding groups.

more than 0.005 Å from the 96-atom results ($AB_{N\perp}$ and $AB'_{N\parallel}$ for Mg-H). In those configurations the 96-atom results are used, as discussed in Sec. V A. Our discussion above made clear that different physical effects are active at BC versus AB_N sites, hence it is not surprising that the corresponding frequencies follow different trends. The linear fits displayed in Fig. 9 match the calculated frequencies to within about 100 cm^{-1} around the fits. It should thus be possible to obtain an estimate of the frequencies solely on the basis of the N-H bond length. For the AB_N configurations (where the largest number of data points is available), the linear fits corresponds to

$$\omega^0 = 3860 - 16164 \times (d_{\text{N-H}} - 1.000), \tag{10}$$

$$\omega = 3768 - 20790 \times (d_{\text{N-H}} - 1.000), \tag{11}$$

where the bond length $d_{\text{N-H}}$ is in Å and the frequencies are in cm^{-1}. We note that the calculated frequencies of NH_3 are also close to the linear fits.

For the harmonic frequency, we can actually attempt an independent prediction of the slope of the linear fit. Indeed, the harmonic frequency should reflect the square root of the curvature of the potential energy curve defined in Eq. (4):

$$\omega^0 = \sqrt{\frac{1}{\mu}\left.\frac{d^2V(x)}{dx^2}\right|_{x=x_0=0}} = \sqrt{\left.\frac{k+6\alpha x}{\mu}\right|_{x=x_0=0}} = \sqrt{\frac{k}{\mu}}. \tag{12}$$

The second derivative of the potential energy curve is equal to $k+6\alpha x$, to first order in x. Now we perturb the oscillator by adding λx to the potential; one can think of this term as a small external force which changes the equilibrium bond length. The equilibrium position is then shifted to $x_0 = -\lambda/k$ (to leading order). We can then find the change of ω^0 with respect to an equilibrium bondlength x_0 as

$$\frac{d\omega^0}{dx_0} = \frac{d}{dx_0}\sqrt{\frac{k+6\alpha x_0}{\mu}} = \frac{6\alpha}{2\mu\omega^0}. \tag{13}$$

Using averaged values of α and ω^0 (from Table VI) and translating the result into our frequency units, we find a slope of -13126 cm^{-1}/Å, in reasonable agreement with the slope of -16164 cm^{-1}/Å derived in Fig. 9. Based on the correlation between vibrational frequencies and N-H bond length evident in Fig. 9 and expressed in Eqs. (10) and (11), one can now derive results for *any* configuration for which the N-H bond length is known.

C. Results for wagging modes

We report our calculated results for vibrational frequencies of N-H wagging modes for some selected configurations. These calculations were carried out in 32-atom cells. These modes of vibration have significantly lower potential energy compared to the bond-stretching modes. The error bar may be slightly larger than ± 100 cm^{-1} here, resulting from the fact that we have to perform calculations using large amplitudes of vibration and resulting in smaller changes in the potential energy. From our preliminary calculations, we found that to obtain potential energy values up to $\frac{3}{2}\hbar\omega$, a wagging amplitude of at least 0.5 Å is required for the BC site and 0.3 Å for the AB_N site. At the same time the frequency (and the potential energy) is up to five times smaller than that of the stretching modes. In order to decouple the bond-stretching mode from the wagging mode, it is imperative to keep the bond distance between N-H fixed. The amplitude of vibration is defined here as the distance along the arc measured from the equilibrium position around the nitrogen atom.[22] We treat the wagging modes as degenerate, although strictly speaking the wurtzite structure breaks the symmetry in the case of the "$\perp$" modes.

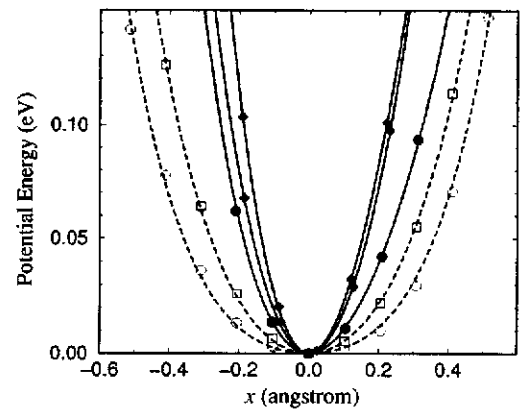

FIG. 10. Calculated potential energy curves for N-H wagging modes for selected configurations. The symbols are calculated points and the lines are the fourth-order polynomial fits [Eq. (4)]. Solid symbols and solid lines indicate AB and OA configurations, while open symbols and dashed lines indicate BC. The potential energies are set to zero at the equilibrium position of each structure. Circles indicate results for isolated interstitial hydrogen, squares for Be-H complexes, and diamonds for Mg-H complexes.

The vibrational frequencies of the wagging modes depend on the configuration and on the stiffness of the N-H bond bending. We could identify no clear trends in the frequency as a function of N-H equilibrium bond length, as we were

TABLE VII. Vibrational properties for H-N wagging modes for selected configurations calculated in 32-atom supercells. $k/2$, α, and β are the second, third, and fourth order coefficients in the polynomial fit of the potential-energy curve [see Eq. (4)], in eV/Å^n, where n is the order of the coefficient. ω^0 is the harmonic component of the vibrational frequency, $\Delta\omega$ is the anharmonic contribution, and ω is the total frequency: $\omega = \omega^0 + \Delta\omega$. Values of ω calculated using perturbation theory [Eq. (5)] are listed in parentheses. All frequencies are in cm^{-1}.

Type	Configuration	$k/2$	α	β	ω^0	$\Delta\omega$	ω
H^+	$BC_\parallel$	0.22	−0.06	1.28	360	153	513 (662)
Be-H	$BC_\parallel$	0.52	−0.10	1.11	549	76	625 (661)
Mg-H	$AB_{N\perp}$	1.87	−0.41	0.86	1040	21	1061 (1061)
H^+	$AB_{N\perp}$	1.15	−1.19	1.71	814	13	827 (821)
Mg-H	$OA_\parallel$	2.45	−2.02	0.78	1190	−33	1157 (1162)

able to do in the case of the stretching modes. We confined our investigations to the wagging modes of the lowest energy configurations for each case (isolated H, Mg-H, and Be-H) plus a few selected configurations. Potential energies as a function of the wagging amplitude (x) are shown in Fig. 10. The symbols indicate data points from our first principles calculations and the lines are the fourth-order polynomial fit to the data points. The fitting parameters as well as resulting frequencies including harmonic and anharmonic terms are tabulated in Table VII.

Both isolated interstitial H^+ and Be-H complexes favor $BC_\parallel$ configurations while Mg-H complexes favor $AB_{N,\perp}$ and $OA_\parallel$. The potential energy curves and frequencies for BC configurations are very different from those for $AB_{N,\perp}$ and $OA_\parallel$. The wagging modes for $AB_{N,\perp}$ and $OA_\parallel$ configurations are consistent with expectations, for instance, based on the symmetric bending mode of NH_3 (at 950 cm^{-1}, Ref. 25). But the BC configurations exhibit much lower frequencies, due to the very shallow nature of the potential in the vicinity of the BC site. Inspection of the potential energy curves reveals, in fact, that the potential energy curve is more U shaped than parabolic; note also the small values of the force constant k in Table VII. A direct comparison is provided by inspection of the potential energy curves in Fig. 10 for isolated interstitial H^+ at BC (solid circles, solid line) versus $AB_{N,\perp}$ (open circles, dashed line).

The $AB_{N,\perp}$ configuration yields a frequency of 827 cm^{-1} for H^+ and 1061 cm^{-1} for Mg-H. The higher frequency for Mg-H is consistent with the increase in the N-H bond strength discussed in Sec. V A when Mg replaces Ga. A similar trend is observed for the stretching mode, see Table VI.

We calculated the wagging mode for Mg-H complexes in the $OA_\parallel$ (solid diamonds in Fig 10). While $OA_\parallel$ does not have the lowest energy, it is the most stable configuration at elevated temperatures due to large entropy associated with its unique structure,[15] as will be discussed in Sec. VI B. The wagging frequency of this configuration was one of the essential ingredients for the entropy calculation. The value (1157 cm^{-1}) is slightly higher than that for $AB_{N,\perp}$ (1061 cm^{-1}), potentially reflecting a stronger interaction with the Mg atom in the $OA_\parallel$ configuration.

Returning to the BC configurations, we observe that the potential energy curves for isolated interstitial H^+ and Be-H complexes at $BC_\parallel$ are symmetric, but highly distorted from parabolic. For the stretching modes, the anharmonic term was negative because the dominant term in $\Delta\omega$ came from the third-order term α, with a smaller correction due to the fourth-order term β [see Eq. (5)]. However, for the BC wagging modes α is very small, and $\Delta\omega$ derives largely from β, resulting in a positive $\Delta\omega$.

Given the large deviation from harmonicity, one might wonder about the accuracy of the perturbation-theory approach (Sec. II B) for deriving the anharmonic frequencies in these cases. Overall, the frequencies calculated using perturbation theory agree remarkably well with the numerical results, as can be seen in Table VII; the deviations are smaller than 40 cm^{-1}. The only exception is the mode for isolated interstitial H^+ in the $BC_\parallel$ configuration, where perturbation theory is off by 150 cm^{-1}, due to β being large and $k/2$ being exceptionally small.

VI. DISCUSSION

A. Comparison with previous computations

Calculations of stable geometries and corresponding energies for H in wurtzite (WZ) and zinc blende (ZB) GaN were reported by Wright,[9] based on DFT in the LDA, and including Ga d states as valence states. For WZ, Wright found the $AB_{N,\perp}$ and $BC_\parallel$ sites to have the same energy, while $BC_\perp$ was higher by 0.16 eV and $AB_{N,\parallel}$ higher by 0.19 eV. These values are in reasonable agreement with our present results. Wright[9] also calculated vibrational frequencies for the stretch modes within the harmonic approximation, finding 3240 cm^{-1} for the $AB_{N,\parallel}$ site, 3120 cm^{-1} for the $AB_{N,\perp}$ site, 3680 cm^{-1} for the $BC_\parallel$ site, and 3480 cm^{-1} for the $BC_\perp$ site. These values are close to our numbers for the harmonic frequencies listed in Table VI. In a subsequent publication,[14] slightly different values were reported: 2970 cm^{-1} for $AB_{N,\perp}$ and 3420 cm^{-1} for $BC_\parallel$; the differences may be due to the use of the actual mass of the H atom rather than a reduced mass in Ref. 14. Reference 14 also provided results for wagging modes, reporting 847 cm^{-1} for $AB_{N,\perp}$ and 502 cm^{-1} for $BC_\parallel$, in good agreement with our results listed in Table VII.

Regarding the comparison between calculations using the *nlcc* and those explicitly including the Ga $3d$ states, we previously[19] performed some explicit tests and extended those in the context of the present study. We found that N-H bond length tend to be slightly shorter when $3d$ states are included, and that the AB_N site tends to be slightly lowered in energy compared to the BC site when $3d$ is compared with *nlcc*. These observations are generally consistent with the differences between Wright's results[9] and ours.

Turning now to the Mg-H complex, in our own previous work[1] we reported a frequency for the AB_N configuration of the Mg-H complex of 3360 cm^{-1}; no anharmonic correction was considered at the time. We note that this frequency agrees very well with the harmonic frequencies listed for $AB_{N,\perp}$ (3333 cm^{-1}) and $AB_{N,\parallel}$ (3335 cm^{-1}) configurations for Mg-H in Table VI, in spite of the fact that the calculations of Ref. 1 were carried out for the zinc blende phase.

Structures and vibrational frequencies for the Mg-H complex in wurtzite GaN have been investigated by Bosin *et al.*,[10] Okamoto *et al.*,[11] Torres *et al.*,[12] Fall *et al.*,[13] and Myers *et al.*[14] None of these studies included anharmonic corrections; a comparison with the harmonic frequency ω^0 is therefore appropriate, although it should be kept in mind that a parabolic fit to data points corresponding to relatively large hydrogen displacements will produce a quadratic term that is lower than the purely harmonic part, i.e., some effect of anharmonicity is probably included even in these calculations. Results from these previous investigations are listed in Table VIII and compared with our present results. The differences between our results and the results of Okamoto *et al.* are likely due to their use of a 16-atom supercell. The agreement

TABLE VIII. Comparison of computational results for Mg-H complexes in wurtzite GaN by various groups. For each set of calculations by a given group, the lowest-energy configuration is listed as zero energy, and ΔE (in eV) is the energy difference with this lowest-energy configuration. Listed frequencies ω^0 (in cm^{-1}) are for vibrational stretching modes, calculated within the harmonic approximation (see Table VI for anharmonic corrections).

Configuration	ΔE (eV)					ω^0 (cm^{-1})				
	Present	Bosin[a]	Okamoto[b]	Torres[c]	Fall[d]	Present	Bosin[a]	Okamoto[b]	Torres[c]	Fall[d]
$AB_{N,\perp}$	0.00	0.00	0.1		0.0	3333	2939			3340
$AB_{N,\parallel}$	0.28	0.47	0.1	0.0	0.2	3335	3069		3277	3580
$BC_{\parallel}$	0.33	0.32	0.0	0.5	>0.3	3859	3611	3490	3645	~4200
$BC_{\perp}$	0.54	0.62	0.0		>0.3		3917	3450		~4200

[a]Reference 10.
[b]Reference 11.
[c]Reference 12.
[d]Reference 13.

with the results of Bosin *et al.* is quite good for the energy differences between different configurations; however, their frequencies seem to be significantly smaller than our present results. This can be attributed to the systematically larger values for N-H bond lengths in their calculations, in spite of the fact that $3d$ states are explicitly included. In addition to the results listed in Table VIII, we mention the frequencies calculated in Ref. 14 for the $AB_{N,\perp}$ configuration: 3284 cm^{-1} for the stretching mode and 937 cm^{-1} for the wagging modes, in good agreement with our results ($\omega^0 = 3333$ cm^{-1} for the stretching mode and 814 cm^{-1} for the wagging modes). Overall, we find reasonable consistency between our present results and previous reports; however, the accuracy of calculated frequencies in the previous work (in particular, the neglect of anharmonic corrections) did not allow for comparisons with experiments at the level of the discussion in the next section.

B. Comparison with experiment

We have obtained results for H in different configurations in isolated interstitial H^+, and in the Mg-H and Be-H complexes. The extent to which, for a given complex, each of these configurations is occupied of course depends on the energy differences between them. For isolated interstitial H^+, the $BC_{\parallel}$ site is favored, with $BC_{\perp}$ and $AB_{N,\parallel}$ only slightly higher in energy. However, the diffusion barrier calculated for H^+ in previous work[1] is only 0.7 eV, and H^+ is thus quite mobile and unlikely to be stable at the interstitial site. Unless experiments are specifically tailored to its observation (e.g., low-temperature proton implantation) we thus do not expect to observe signals related to isolated interstitial H. We point out that because we explicitly report harmonic and anharmonic terms, our calculated values for H can be easily used to derive values for D, using the approach described in Sec. II C.

In the Be-H complex, the BC sites are overwhelmingly favored. Experimental observations have not yet been reported; we thus offer our calculated frequency as a prediction. We obtained 3299 cm^{-1} for the stretching mode and 625 cm^{-1} for the wagging modes.

A number of experimental studies have been carried out for Mg-H complexes in GaN. Our total energy calculations indicate that the $AB_{N,\perp}$ site is favored, but the other configurations are only slightly higher in energy (see Table IV); in particular, we focused on the $OA_{\parallel}$ which will turn out to be very relevant. It then becomes very interesting to compare our calculated frequencies with experiment. The differences between the calculated stretching-mode frequencies for the $AB_{N,\perp}$, $OA_{\parallel}$, and $AB_{N,\parallel}$ configurations are smaller than the error bar of our calculations: we obtain ω=3045,3068, and 3113 cm^{-1}, respectively (Table VI). The harmonic frequencies ω^0 are even closer. The similarity in the frequencies is of course related to the almost identical N-H bond lengths in all three configurations, as discussed in Sec. V B. In contrast, the calculated frequency for the BC configuration is much higher, at 3742 cm^{-1}; however, we remind the reader that the BC configuration is not even metastable for Mg-H (see Sec. IV B).

As mentioned in the Introduction (Sec. I), the local vibrational mode of the Mg-H complex has been experimentally determined to occur at 3125 cm^{-1}).[4–6] The measured frequency agrees within our error bar with our calculated frequencies for the $AB_{N,\perp}$, $OA_{\parallel}$, or $AB_{N,\parallel}$ configurations.

The experiments of Götz *et al.*[4] actually provided another useful piece of information, namely, the frequency for the stretching mode in the Mg-D complex. This line was found at 2321 cm^{-1}. We can go through the formalism outlined in Sec. II C, and use Eqs. (6), (7), (8), and (9). The reduced massed in this case are simply those for a N-H (or N-D) oscillator, i.e., $\mu_H = 0.933\ m_H$ and $\mu_D = 1.75\ m_H$. We thus obtain the following values: $\omega_H^0 = 3324$ cm^{-1} and $\Delta\omega_H = -199$ cm^{-1}. For the reasons outlined in Sec. II C, the anharmonic term determined in this fashion has a sizable error bar, because it is very sensitive to the ratio of the reduced masses. However, the values derived here are certainly in reasonable agreement with our calculated values of ω^0 and $\Delta\omega$ (Table VI), the large magnitude of $\Delta\omega$ again emphasizing that anharmonic contributions are very important in this system.

We concluded above that, based on calculated frequencies alone, we cannot distinguish between the $AB_{N,\perp}$, $OA_{\parallel}$, and

$AB_{N,\parallel}$ configurations. Fortunately, the infrared spectroscopy experiments of Clerjaud *et al.*[6] provided additional information about the Mg-H complex. By using polarized light they were able to determine that the complex was *not* aligned along the c axis. This agrees with our calculations, which show that "$\parallel$" configurations ($AB_{N,\parallel}$, $BC_{\parallel}$, and $AB'_{N,\parallel}$) are higher in energy (see Table IV). Clerjaud *et al.* also derived the angle between the c axis and the electric dipole induced by the mode, finding a value of $\theta=130\pm5°$. Since hydrogen exhibits the largest displacement amplitude in the 3125 cm^{-1} mode, it is natural to assume that the angle θ reflects the direction of the N-H bond length. The experimental result $\theta=130°$ is therefore not consistent with the $AB_{N,\perp}$ configuration, in which the angle θ is very close to 109° (see Fig. 5). Figure 5 shows, however, that the $OA_{\parallel}$ configuration exhibits an angle of 134°, in very good agreement with experiment. Note that the $OA_{\perp}$ configuration, in which the N-H bond angle deviates from 109° in the opposite direction, can be safely excluded as a candidate for the experimentally observed structure.

The agreement between the observations of Clerjaud *et al.*[6] and our calculated structure seems to provide a compelling argument for concluding that the microscopic structure corresponds to the $OA_{\parallel}$ configuration. However, as we see in Table IV, this configuration is *not* the lowest-energy structure for the Mg-H complex; the "regular" $AB_{N,\perp}$ complex (with an angle $\theta=109°$) is lower in energy by 0.19 eV. The resolution to this puzzle is provided by a thorough investigation of temperature-dependent effects, as reported in Ref. 15. It turns out that the $OA_{\parallel}$ configuration gives rise to a set of low-energy excitations, which contribute significantly to the *entropy* of the complex. Our studies show that it costs very little energy to move H away from the $OA_{\parallel}$ position, maintaining the "polar" angle θ with the c axis and rotating H around the c axis [see Fig. 5(b)]. The entropy associated with this nearly free rotation plays an essential role in stabilizing the complex. The rotational excitation spectrum was calculated using a quantum-mechanical model in which the hydrogen atom moves in a weak corrugation potential, and the resulting free energies were obtained by evaluating the partition function.[15] At sufficiently high temperatures the entropy term lowers the free energy of the $OA_{\parallel}$ configuration below that of $AB_{N,\perp}$. Both energetic and structural arguments thus favor the $OA_{\parallel}$ configuration as the microscopic structure of the Mg-H complex observed in Refs. 4–6.

VII. SUMMARY

We have presented first-principles calculations of energetics and vibrational frequencies for various configurations assumed by hydrogen in p-type GaN. The main results are summarized in Table I. We have shown that it is very important to go beyond the harmonic approximation and take anharmonic contributions into account, due to the light mass of the hydrogen atom. Our approach has been to fit the calculated potential energy values to a fourth-order polynomial and calculate the vibrational frequencies by explicit numerical solution of the Schrödinger equation. Perturbation theory provides a simpler and reasonably accurate alternative. We also investigated the trends in stretching-mode frequencies, finding a strong correlation with the length of the N-H bond. For the important Mg-H complex, we found very similar stretching-mode frequencies for three configurations ($AB_{N,\perp}$, $OA_{\parallel}$, and $AB_{N,\parallel}$), all in good agreement with the experimental value.[4–6] Additional information about the orientation of the N-H bond in this complex[6] allows us to identify $OA_{\parallel}$ as the microscopic structure. We also found this configuration to be most stable at high temperatures.[15] Predictions for Be-H complexes and for isolated interstitial H^+ in GaN will be useful for identification of the microscopic structure of the species responsible for vibrational modes in future infrared or Raman spectroscopy experiments.

ACKNOWLEDGMENTS

This work was supported by the Air Force Office of Scientific Research, Contract No. F4920-00-C-0019, monitored by G. Witt, and by the Office of Naval Research, Contract No. N00014-99-C-0161, monitored by C. Wood. We thank N. M. Johnson, M. D. McCluskey and J. Neugebauer for useful discussions and suggestions. C.VdW. is grateful to the Fritz-Haber-Institut and Paul-Drude-Institut, Berlin, for their hospitality, and to the Alexander von Humboldt Foundation for a *US Senior Scientist Award*.

*Current address: School of Physics, Institute of Science, Suranaree University of Technology, Nakhon Ratchasima, Thailand.

[1] J. Neugebauer and C. G. Van de Walle, Phys. Rev. Lett. **75**, 4452 (1995).

[2] S. Nakamura, N. Iwasa, M. Senoh, and T. Mukai, Jpn. J. Appl. Phys. **31**, 1258 (1992).

[3] J. Neugebauer and C. G. Van de Walle, Appl. Phys. Lett. **68**, 1829 (1996).

[4] W. Götz, N. M. Johnson, D. P. Bour, M. D. McCluskey, and E. E. Haller, Appl. Phys. Lett. **69**, 3725 (1996).

[5] H. Harima, T. Inoue, S. Nakashima, M. Ishida, and M. Taneya, Appl. Phys. Lett. **75**, 1383 (1999).

[6] B. Clerjaud, D. Côte, A. Lebkiri, C. Naud, J. M. Baranowski, K. Pakula, D. Wasik, and T. Suski, Phys. Rev. B **61**, 8238 (2000).

[7] J. Neugebauer and Chris G. Van de Walle, J. Appl. Phys. **85**, 3003 (1999).

[8] C. G. Van de Walle, S. Limpijumnong, and J. Neugebauer, Phys. Rev. B **63**, 245205 (2001).

[9] A. F. Wright, Phys. Rev. B **60**, 5101 (1999).

[10] A. Bosin, V. Fiorentini, and D. Vanderbilt, in *Gallium Nitride and Related Materials*, edited by F.A. Ponce *et al.*, Mater. Res. Soc. Symp. Proc. Symposia Proceedings No. 395 (Materials Research Society, Warrendate, PA, 1996), p. 503.

[11] Y. Okamoto, M. Saito, and A. Oshiyama, Jpn. J. Appl. Phys. **35**, L807 (1996).

[12] V. J. B. Torres, S. Öberg, and R. Jones, MRS Internet J. Nitride Semicond. Res. **2**, 35 (1997).

[13] C. J. Fall, R. Jones, P. R. Briddon, and S. Öberg, Mater. Sci. Eng., B **82**, 88 (2001).

[14] S. M. Myers, A. F. Wright, G. A. Petersen, C. H. Seager, W. R. Wampler, M. H. Crawford, and J. Han, J. Appl. Phys. **88**, 4676 (2000).
[15] S. Limpijumnong, J. E. Northrup, and C. G. Van de Walle, Phys. Rev. Lett. **87**, 205505 (2001).
[16] P. Hohenberg and W. Kohn, Phys. Rev. B **136**, B864 (1964); W. Kohn and L. J. Sham, *ibid.* **140**, A1133 (1965).
[17] M. Bockstedte, A. Kley, J. Neugebauer, and M. Scheffler, Comput. Phys. Commun. **107**, 187 (1997).
[18] S. G. Louie, S. Froyen, and M. L. Cohen, Phys. Rev. B **26**, 1738 (1982).
[19] J. Neugebauer and C. G. Van de Walle, in *Defect and Impurity Engineered Semiconductors and Devices*, edited by S. Ashok *et al.*, Mater. Res. Soc. Symp. Proc. Symposia Proceedings No. 378 (Materials Research Society, Warrendate, PA, 1995), p. 503.
[20] H. J. Monkhorst and J. D. Pack, Phys. Rev. B **13**, 5188 (1976).
[21] C. G. Van de Walle, Phys. Rev. Lett. **80**, 2177 (1998).
[22] S. Limpijumnong and C. G. Van de Walle, in *GaN and Related Alloys*, edited by U. Mishra, M.S. Shur, C.M. Wetzel, B. Gil, and K. Kishino, MRS Symposia Proceedings No. 639 (Materials Research Society, Pittsburgh, 2001), p. G4.3.
[23] The term "global minimum" is used to describe the lowest-energy configuration amongst the local minima that resulted from our study. Because of the large amount of calculations performed (only a subset of which has been explicitly reported here), using different starting positions for the atoms and always allowing atomic relaxation, we are quite confident that we have identified the global minima. Still, there is a remote possibility that a lower-energy configuration may have been overlooked.
[24] L. D. Landau and E. M. Lifshitz, *Quantum Mechanics* 3rd ed. (Pergamon, Oxford, 1977), p. 136.
[25] *CRC Handbook of Chemistry and Physics*, 73rd ed., edited by David R. Lide (CRC Press, Boca Raton, 1992), pp. 9–20 and 9–149.
[26] http://srdata.nist.gov/cccbdb/; The vibrational frequencies included in this range are chosen from those calculations that give a reasonable bond distance, i.e., within 1% of experiment.
[27] *Periodic Table of the Elements* (Sargent-Welch, Buffalo Grove, IL, 1980).